UDC 551.509.61:551.515.21:551.509.313:551.511.33

A CIRCULARLY SYMMETRIC PRIMITIVE-EQUATION MODEL OF TROPICAL CYCLONES AND ITS RESPONSE TO ARTIFICIAL ENHANCEMENT OF THE CONVECTIVE HEATING FUNCTIONS

STANLEY L. ROSENTHAL

National Hurricane Research Laboratory, Environmental Research Laboratories, NOAA, Miami, Fla.

ABSTRACT

Simulations of the natural (unmodified) evolution of tropical cyclones with a circularly symmetric model suggest that seeding of hurricanes with silver iodide at radii greater than that of the surface wind maximum might be more effective in decreasing the surface wind maximum than seedings at or within the wind maximum. Seeding simulations with the model strongly suggest that the model storm responds in the sense anticipated. On the other hand, simulated seedings at radii less than that of the surface wind maximum produce temporary increases in the strength of the maximum. However, termination of the seeding is followed by a rapid recovery of the modified storm to a state close to that of the control.

1. INTRODUCTION

Over the past few years, a primitive equation model that simulates the development of tropical cyclones and their structure with a fair degree of reality hsa been developed at NHRL (National Hurricane Research Laboratory, Rosenthal 1970*a*, 1970*b*). While the primary motivation for this work has been increased understanding of hurricane dynamics, we have also realized that such a model would have some value for testing and evaluating various experiments suggested for trial in hurricane modification. An early and extremely crude version of the model (Rosenthal 1969) was used in 1968 to simulate the seeding of the hurricane wall cloud by silver iodide. Some of these results have already been published (Gentry 1969).

The calculations were aimed at testing a variant of the hypothesis by Simpson and Malkus (1964). Simpson and Malkus recognized that the hurricane wall cloud is located quite close to the region of maximum low-level pressure gradient and further contended that the wall cloud contains significant quantities of supercooled water. According to the hypothesis, if this supercooled water were frozen through nucleation by silver iodide crystals, the released heat of fusion would produce temperature increases; and therefore, hydrostatically, pressure decreases near the region of the strongest pressure gradient would shortly be realized. If the central pressure did not concomitantly decrease, a reduction in pressure gradient and, in turn, a reduction in wind speed should be the net result.

Through the years, this hypothesis has been subjected to considerable criticism (largely unpublished). Some of the critics have argued that the sense of the reaction would be different from that proposed. Others have conceded the hypothesized chain of events but have contended that its magnitude would be undetectable within the background of the hurricane's natural short-range variability.

The few numerical experiments carried out prior to the 1968 seeding simulations suggested that a slight variant of the Simpson-Malkus proposal might be worthy of consideration. These calculations showed that, during intensification of the model storm, maximum heating (normally associated with the eye wall) was located at a significantly smaller radius than the surface wind maximum. As development proceeded, the wind maxima moved inward more rapidly than did the heating maxima. Invariably, development ceased and decay commenced when the heating maxima and the surface wind maximum became nearly coincident. The implication of this sequence of events, at least for the model storm, is that heating at radii less than that of the surface wind maximum is favorable for intensification and that the reverse is true for heating at radii greater than that of the surface wind maximum.

The seeding simulations reported on in 1969 seemed to verify this notion. When the "seeding" was done at radii greater than that of the surface wind maximum, we found decreases in intensity of greater magnitude and of longer duration than those observed when the seeding crossed the maximum winds (Gentry 1969). In both cases, however, the seeding was at radii greater than that of the strongest "natural" heating. The results of these calculations were used as guidance material for planning the 1969 Project STORMFURY field experiments (Gentry 1969).

A substantial difficulty in the interpretation of the calculations arose from the fact that the control calculation never attained a reasonably steady state (as measured by either central pressure or the surface wind maximum). Rather, it reached peak intensity and decayed fairly rapidly thereafter (see fig. 1 in Rosenthal 1969). Detailed examination (at 10-min intervals) near the time of greatest intensity showed oscillations in the surface wind maximum with a period of 3–4 hr and an amplitude of about 1.5 m/s (fig. 2 in Gentry 1969). In comparison to the control, the seeded storms showed decreases in intensity

that started as soon as the seeding began. The duration of this decreased intensity was between 1.5 and 4 hr, depending upon the radii at which the seeding was performed. Measured by winds at the surface, the magnitude of the decrease was about 2 m/s. However, the overall impression obtained from viewing the results was that of a phase change of the temporal oscillations. The amplitudes of the oscillations in the seeded storms were not noticeably different from those of the control.

These calculations were intended to simulate "single seeding" field experiments in which the seeder aircraft discharges its material once in a pass of 2–3 min covering a radial interval of about 30 km. The feeling of those involved in the field program (Gentry 1969) was that a single-seeding experiment could release heat of fusion over the 500- to 300-mb layer equivalent to a heating rate of 2°C/30 min and lasting for a period of 30 min. At 300 mb, this amounts to freezing about 2.5 g water$\cdot m^{-3} \cdot 30 min^{-1}$. At 500 mb, the figure is approximately 4 g water$\cdot m^{-3} \cdot 30$ min^{-1}. While the release of silver iodide is made along a particular azimuth, those involved in the field program feel that the circulation of the storm sweeps the material in a more or less circular path, thus providing the heating rates cited above in a circular fashion.

For simulating this process, the heating function that represents the cumulus feedback on the macroscale (Rosenthal 1969) was simply increased by the amount and for the period cited above at selected radii.

The author is well aware that substantial uncertainty exists concerning the "true" heat of fusion released in such experiments and recognizes the obvious need for increased observational and experimental efforts aimed at establishing these freezing rates. Because of this uncertainty, because of the extremely crude manner in which the seeding is simulated, and because of other reasons to be cited later, results obtained from the model must not be taken too literally. We do not contend that the model conditions are found in the real atmosphere. Rather, we stipulate hypothetical conditions and ask the model to determine the theoretical consequences of these conditions. *At best, the results should be considered qualitative guidance material.*

By August 1969, the design of the field experiment (Gentry 1970) had been altered such that single seedings (as previously defined) were repeated five times at 2-hr intervals at radii for which selection was partially based on the results of the calculations already described. Since the model had been substantially improved by this time and since no simulations of multiple-seeding experiments had as yet been carried out, the new series of calculations, discussed below, were performed.

2. REVIEW OF THE MODEL

With the exceptions cited in this paragraph, the version of the model used for the 1969 seeding simulations is identical to that described by Rosenthal (1970*b*). The original model simulated the air-sea exchanges of sensible and latent heat through the requirement that temperature and relative humidity at the lowest two levels (1015 and 900 mb) be steady state and horizontally uniform. This pragmatic restraint is still present in the calculations discussed by Rosenthal (1970*b*). However, by November 1969 when the new seeding simulations were performed, the program had been generalized to include explicit predictions of the air-sea exchanges of sensible and latent heat.

Despite the fact that this model is one of the more sophisticated of the circularly symmetric models in existence and despite the fact that it has provided extremely realistic results (Rosenthal 1970*b*), it does suffer from two major deficiencies. The first of these is the highly pragmatic parameterization of cumulus convection (Rosenthal 1970*b*). Substantial improvements in this area must await increased understanding of both cumulus convection and its interaction with macroscale flows.

The second major difficulty comes from the assumption of circular symmetry and precludes direct comparison between model calculations and specific real tropical cyclones. The latter are strongly influenced by interactions with neighboring synoptic systems, and these vary markedly in character from storm to storm. The model results must, therefore, be considered as representative of some sort of average cyclone. Despite this, however, a companion paper by one of the author's colleagues (Hawkins 1971) does make some interesting comparisons between the seeding simulations described below and the field experiment. These comparisons show a number of areas in which the model behaves in a fashion similar to the observed behavior of hurricane Debbie. There also are, of course, areas in which the model calculation and the field experiment show significant differences.

3. THE CONTROL EXPERIMENT

The major characteristics of the control selected (experiment S18) are summarized below and differ from one already published (exp. W1, Rosenthal 1970*b*) only in the more general treatment of air-sea exchanges of sensible and latent heat as described in the previous section.

Figure 1 summarizes the sea-level history of experiment S18. Deepest central pressure and strongest winds occur at 168 hr. These peaks, however, appear to represent "overshooting" of an equilibrium state; and as is shown below, a closer approach to a steady state is found between 192 and 216 hr. As we have noted previously (Rosenthal 1969, 1970*a*, 1970*b*), the vertical motion at 900 mb is an excellent measure of the convective heating in the model. From the bottom section of figure 1, therefore, it is clear that the relationship between the radius of maximum heating and that of the strongest surface winds is as described in section 1 (i.e., during the growth stage, strongest heating is at a radius smaller than that of the strongest surface winds). After maximum intensity is reached, the inverse appears to be the case.

421-361 O—71——6

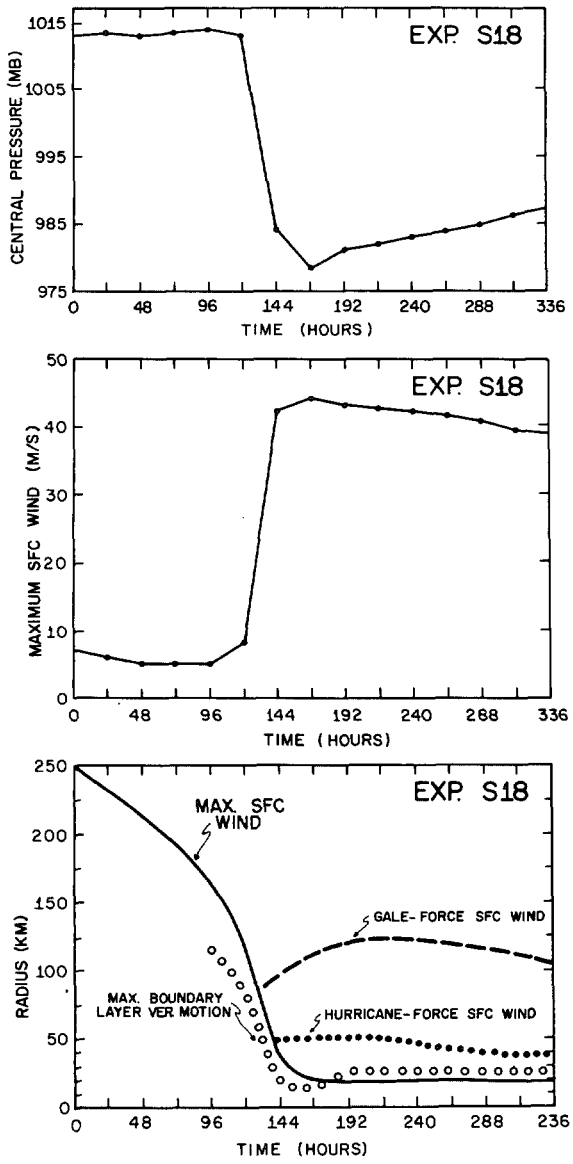

FIGURE 1.—Results from experiment S18.

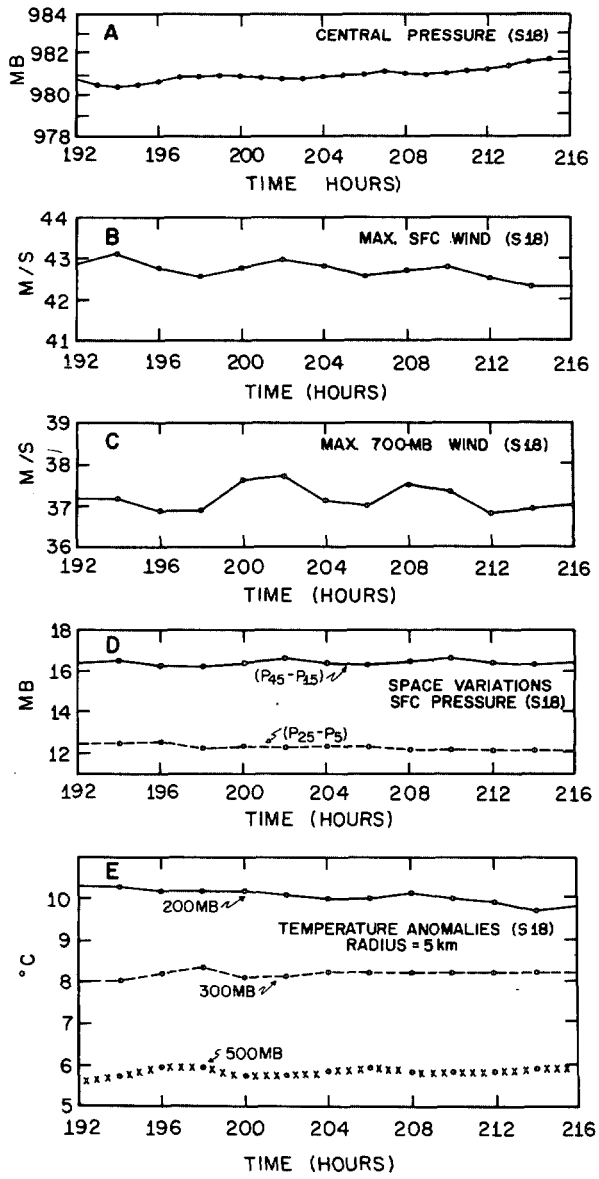

FIGURE 2.—Results from experiment S18; time histories of (A) central pressure, (B) maximum surface wind, (C) maximum 700-mb wind, (D) surface pressure differences between 45 and 15 km and between 25 and 5 km, (E) temperature anomalies at 5-km radius.

Figure 2 shows detailed histories of several variables during the 192- to 216-hr period and verifies the near-steady state of the model storm during this interval. The net change in central pressure is less than 1 mb while the surface wind maximum changes by less than 1 m/s. An oscillation with a period of about 8 hr appears in the data, but the amplitude is quite small. In the 700-mb winds where the amplitude appears greatest, it is less than 0.5 m/s.

Figures 3 through 6 provide additional information concerning the structure of the model storm at hour 192 but may be considered representative of the entire period of 192–216 hr.

4. PROCEDURES FOR THE SEEDING SIMULATIONS

The heating rates for the seeding simulations were established after discussion with Dr. Gentry (NHRL). These consultations revealed that he continued in his belief that 2°C/30 min was the correct heating rate for a single seeding. However, he was now of the opinion that the effect would be felt for at least 1 hr (in contrast to the 0.5 hr cited at the time of the 1968 calculations). It was also Dr. Gentry's feeling that the enhanced heating might be more or less continuous over the 10-hr period spanned by the multiple-seeding operation. As in the case of the 1968 calculations, results produced by seeding at different radii were compared. We also attempted to determine the effect of heating rates larger than those cited above.

Calculations with the larger heating rates were performed primarily as a matter of theoretical interest and certainly are not intended to imply that such heating rates can be realized over circular rings of the size treated here. As already noted, substantial observational effort is

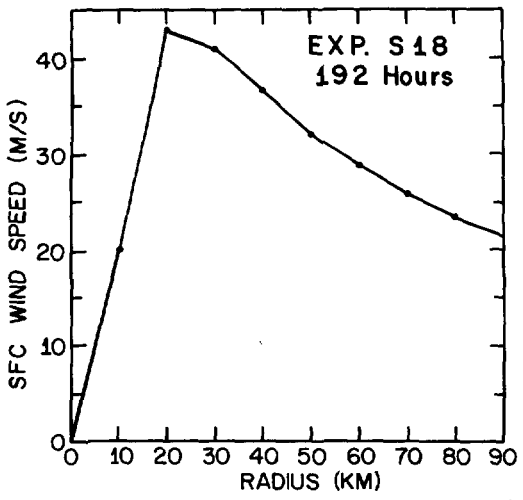

FIGURE 3.—Results from experiment S18; radial profile of surface wind speed at 192 hr.

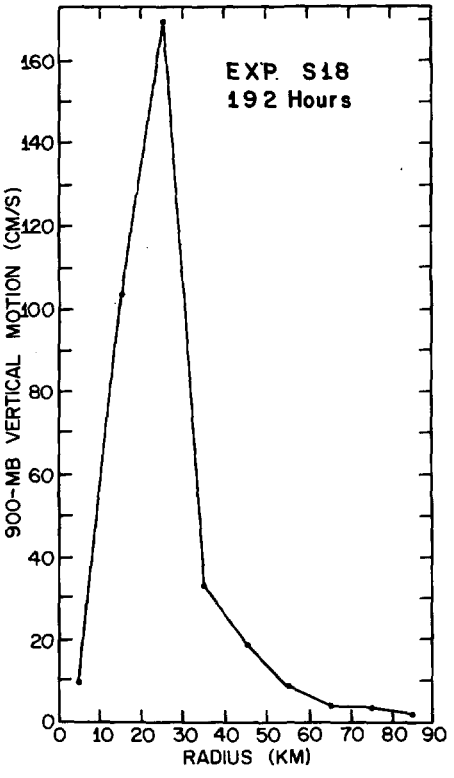

FIGURE 4.—Results from experiment S18; radial profile of 900-mb vertical motion at 192 hr.

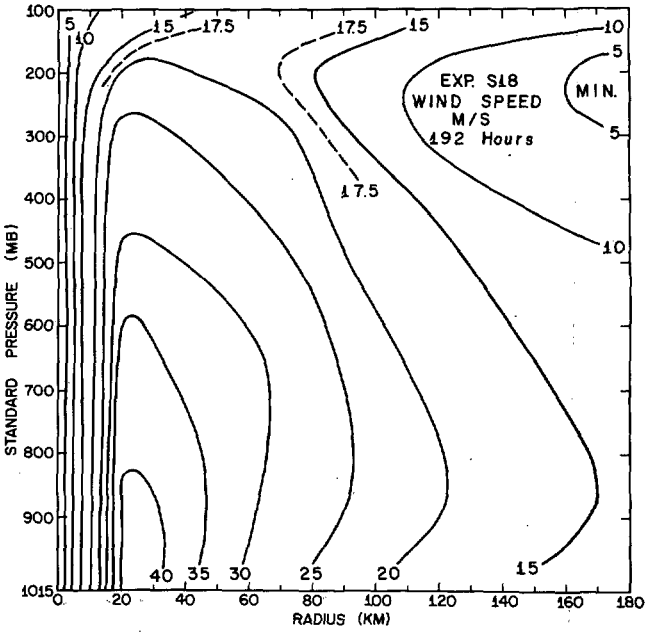

FIGURE 5.—Results from experiment S18; cross section of total wind speed at 192 hr.

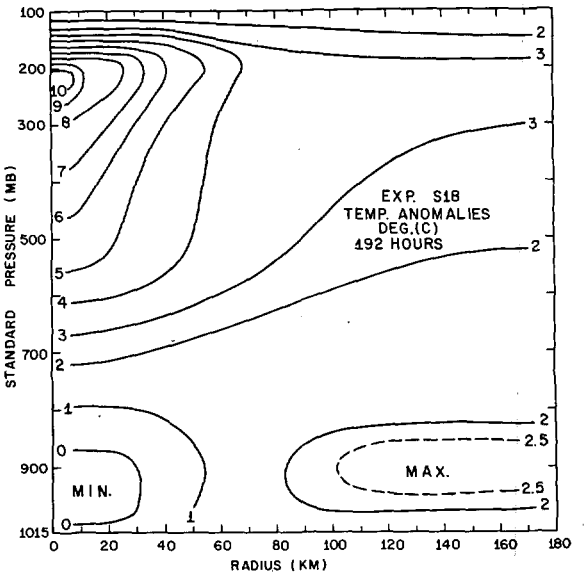

FIGURE 6.—Results from experiment S18; cross section of temperature anomaly at 192 hr.

required before the heating rates realized in the field program can be firmly established.

The seeding simulations may be distinguished from each other, therefore, on the basis of three characteristics:

1. Whether the enhanced heating function was applied continuously or intermittently.
2. The radii at which the enhanced heating was applied.
3. The magnitude of the enhanced heating.

As was the case for the 1968 calculations, the heating function is enhanced only at the 300- and 500-mb levels, which are the levels in the model within the layer seeded in the field experiment. For enhanced heating of the intermittent type, the heating functions were increased during hours 192–193, 194–195, 196–197, 198–199, and 200–201. For continuous enhanced heating, the heating function was increased by a fixed amount over the period 192–202 hr. Differences between calculations with continuous and intermittent enhancement are relatively minor. As a consequence, results shown are primarily for cases of continuous heating.

Experiments in which the seeding radii are varied are distinguished by the terms "small" and "large" radii experiments. In the small radii experiments, heating is enhanced at 25, 35, and 45 km. The natural heating is

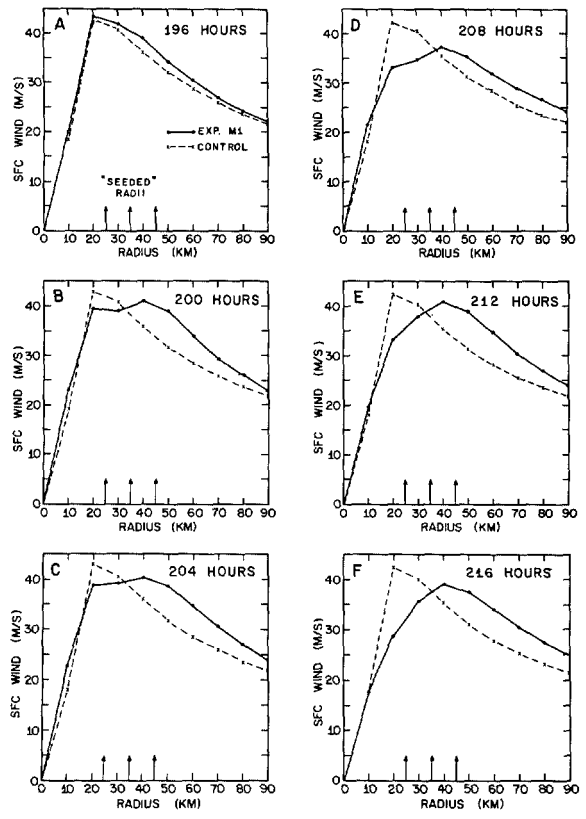

FIGURE 7.—Results from experiment M1; comparison of surface wind profiles with the control experiment S18 as a function of time; arrows indicate grid points at which enhanced heating was applied.

greatest at 25 km (fig. 4), so these calculations contain enhanced heating at the natural maximum as well as at the next two grid points with larger radii. In large radii experiments, heating is enhanced at 35, 45, and 55 km, clearly beyond the radius of largest natural heating. In both types of experiments, enhanced heating is at radii larger than that of the surface wind maximum (cf. figs. 3 and 4).

Experiments in which the magnitude of the enhanced heating is varied are referred to as "normal," "large," and "extreme" heating cases. In the normal heating experiment, the heating function is increased by an amount equivalent to 2°C/30 min. For large and extreme heating experiments, the enhancement is by 6°C/30 min and 18°C/30 min, respectively.

5. CONTINUOUS NORMAL HEATING AT SMALL RADII (EXP. M1)

Figure 7 depicts the comparison of surface wind profiles with the control experiment. During the first 4 hr of enhanced heating, the surface winds tend to become slightly more intense than the control, particularly at radii just beyond the center of the seeded region. After 8 hr of enhanced heating (fig. 7B), a new surface wind maximum has formed at 40 km, and the wind has decreased by about 3 m/s at the radius of the original maximum. At the new maximum, the wind is about 5 m/s greater than the control; and beyond 30 km, the modified storm is everywhere more intense than the control. At 204 hr (fig. 7C), which is 2 hr after the termination of the enhanced heating, the new maximum has become slightly less intense (by about 0.5 m/s) and continues to decrease in intensity (as do all the winds between radii of 20 and 70 km) until 208 hr. This is undoubtedly a result of the storm having come into some sort of balanced state with the enhanced heating which is then upset when the seeding is terminated. At 208 hr at the radius of the original maximum, the modified storm shows surface winds less than that of the control by about 10 m/s. The maximum of the modified storm (at 40-km radius) is about 5 m/s less than the maximum for the control. Substantial portions of the seeded storm, however, continue to show winds stronger than those of the control.

Figures 7D–7F show the new wind maximum at 40 km to be a stable feature of the modified storm. The decrease in intensity noted between 204 and 208 hr does not continue indefinitely, and the system appears to oscillate in an attempt to find a new equilibrium. At 216 hr, winds at the 20-km radius are about 14 m/s less than those of the control. However, the maxima for the two experiments differ only by about 3.5 m/s.

At 700 mb (fig. 8), intensification during the first 4 hr is significantly greater than at the surface, presumably due to the absence of the moderating effects of surface drag. By 200 hr, a new 700-mb wind maximum is established at 50 km; and in contrast to conditions at sea level, the new maximum is stronger [1] (by about 3.5 m/s) than that of the control. At the radius of the new maximum, 700-mb winds are about 10 m/s greater than those of the control. While the sense of the evolution of the 700-mb data is more or less similar to that found at the surface, only at 208 hr (6 hr after the termination of the enhanced heating) is the maximum in the modified storm less than that of the control.

In summary, figures 7 and 8 show the evolution of the wind field to be in some degree similar to that predicted by the slight variant of the Simpson-Malkus hypothesis suggested in section 1. The surface wind maxima do establish themselves in fairly stable configurations at larger radii and with less intensity. However, beyond 30 to 40 km, surface winds become more intense than those of the control. When the enhanced heating is terminated, winds tend to decrease. However, this decrease is not persistent; and the modified storm oscillates apparently in an attempt to find a new balanced state. The evolution at 700 mb is similar; but here, the initial intensification is greater, and during most of the calculation the 700-mb wind maximum is stronger than that of the control. Moreover (see footnote 1), the latter factor may be due to grid spacing.

The histories of these wind maxima as well as that of the central pressure are summarized in figure 9. The central pressure decreases during the period of the enhanced heating, begins to increase only after the seeding is terminated, and even then is never more than about

[1] The configuration of the control 700-mb profile indicates that, with finer resolution, the results at this level might change significantly. On the other hand, the radial resolution at the surface appears to be adequate.

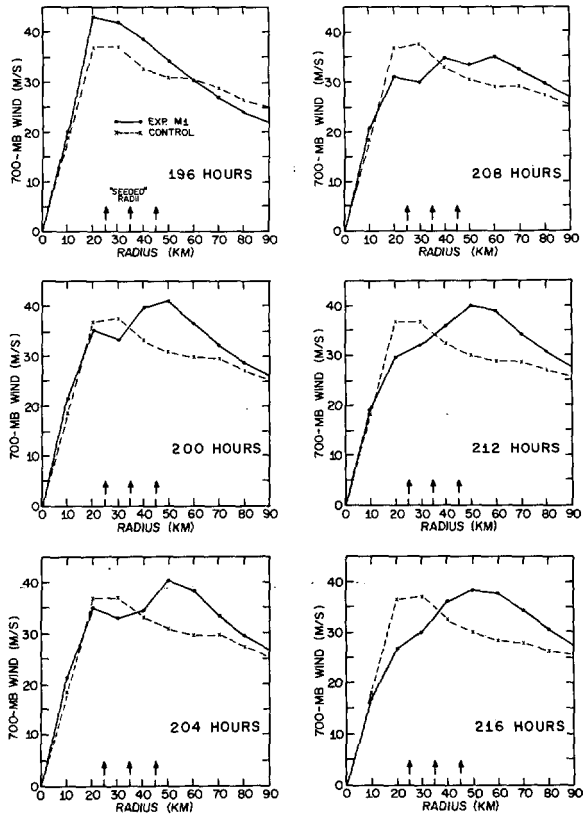

FIGURE 8.—Results from experiment M1; comparisons of 700-mb wind profiles with those for the control experiment S18 as a function of time; arrows indicate grid points at which enhanced heating was applied.

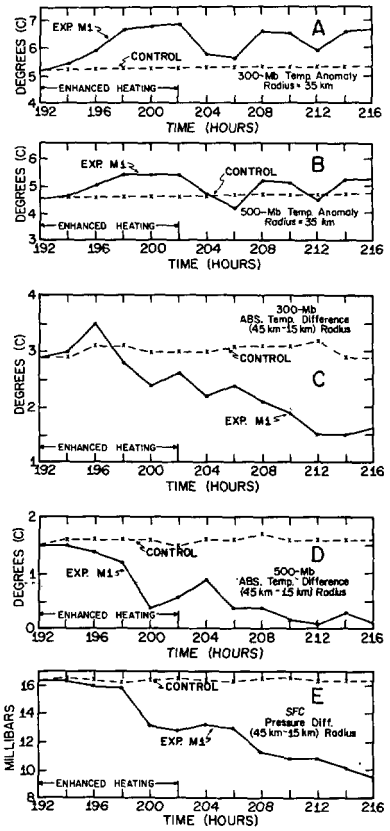

FIGURE 10.—Comparisons of time histories of experiment M1 with those of the control experiment.

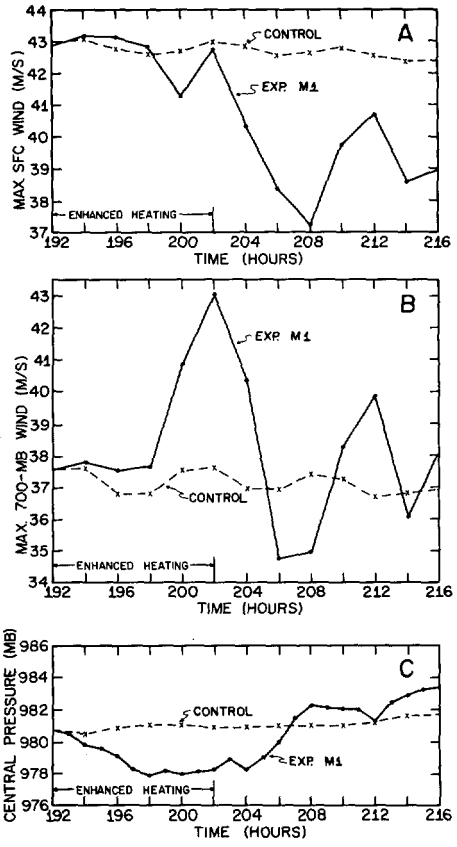

FIGURE 9.—Comparisons of time histories of experiment M1 with those of the control experiment; (A) surface wind maxima, (B) 700-mb wind maxima, (C) central pressure.

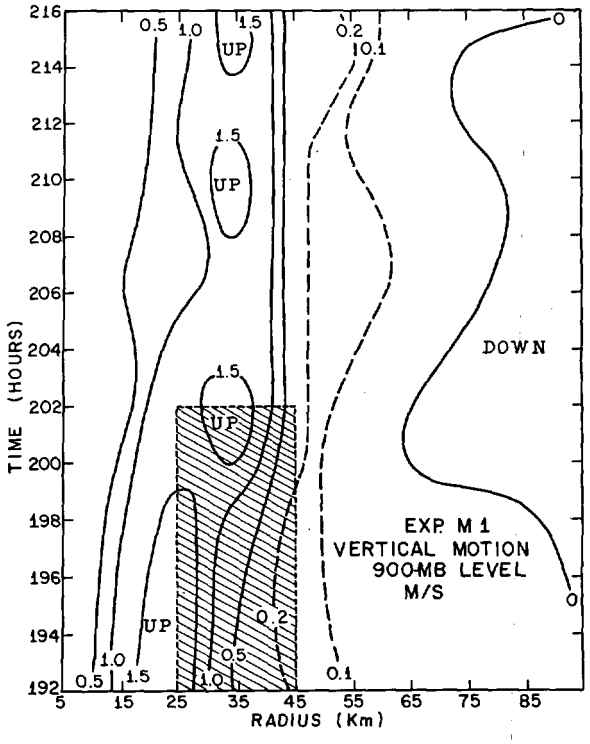

FIGURE 11.—Results from experiment M1; time-radius cross section of 900-mb vertical motion.

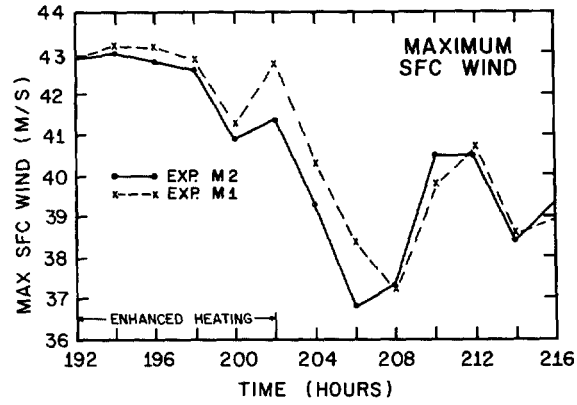

FIGURE 12.—Time histories of surface wind maxima for experiments M1 and M2.

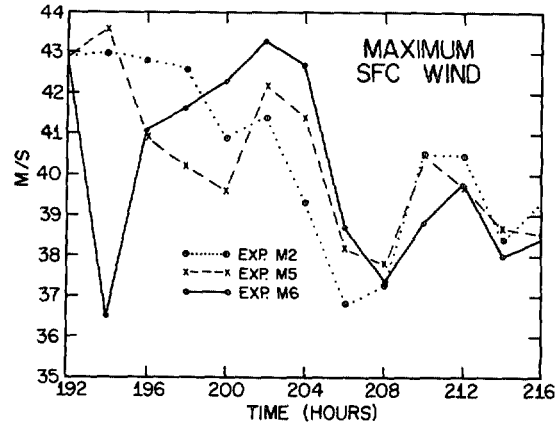

FIGURE 13.—Time histories of the surface wind maxima for experiments M2, M5, and M6.

1.5 mb greater than the control. The evolution of the 300- and 500-mb temperatures (figs. 10A and 10B) at the midpoint of the seeded region (35-km radius) show rather small increases that never exceed 2°C. The radial temperature gradients, however, are reduced substantially (figs. 10C and 10D); and the surface pressure gradient is correspondingly reduced (fig. 10E).

Figure 11 shows that the maximum low-level vertical motion shifts outward to a radius of 35 km and increases slightly in strength until the enhanced heating is terminated. Thereafter, it remains fixed at the new location while oscillating in magnitude.

6. CONTINUOUS NORMAL HEATING AT LARGE RADII (EXP. M2)

Experiment M2 was also conducted with normal and continuous heating, but the enhancement was at large radii. Figure 12 shows that, at the normal heating rate, the differences produced by heating enhancement at small and large radii are small but in the sense predicted by the arguments of section 1. Nevertheless, even at their largest, the differences in maximum winds between the two experiments are only about 1 m/s.

7. EXPERIMENTS WITH EXTREME HEATING

Two experiments are of prime interest in this section:

1. Experiment M5 (continuous extreme heating at small radii).
2. Experiment M6 (continuous extreme heating at large radii).

Figure 13 shows a comparison of surface wind maxima for these calculations with those for experiment M2. A surprising aspect of the figure is the tendency for the three results to approach each other near the end of the calculations, despite the fact that enhanced heating in experiments M5 and M6 is nine times that for M2. The major differences are in the first few hours when the strength of the wind maximum for M6 (extreme heating, large radii) decreases dramatically and then increases in an equally dramatic fashion. The surface wind profiles for experiment M5 behave very much like those for M1 and

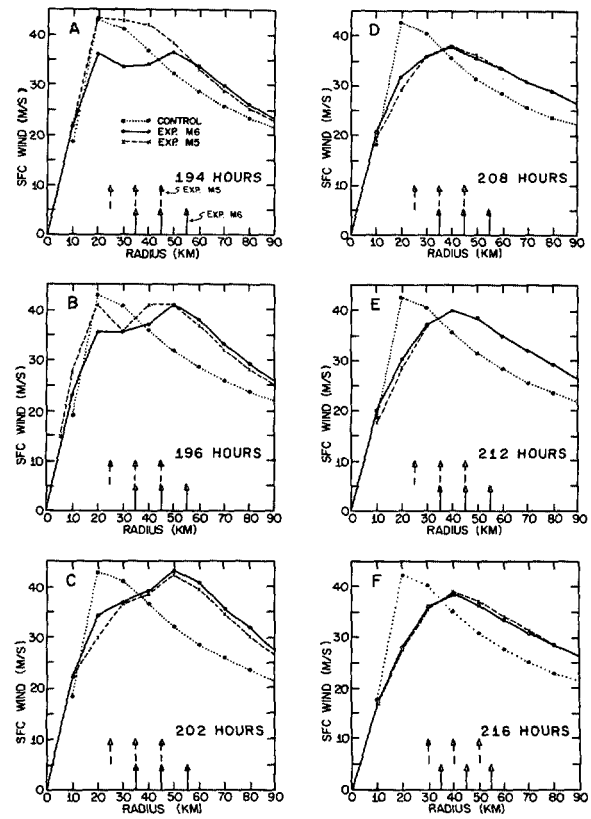

FIGURE 14.—Comparisons of surface wind profiles for experiment M5, experiment M6, and the control experiment as a function of time; arrows indicate grid points at which enhanced heating was applied.

M2 (fig. 14). In M6, however, the original surface wind maximum is destroyed very rapidly. The sharp reduction in surface wind at 194 hr of M6 (fig. 13) represents a transition period in which the original maximum has been weakened and the new maximum has not as yet become well established. However, by 202 hr when the enhanced heating is terminated and thereafter, experiments M5 and M6 provide results that are much the same (figs. 14C–14F). Beyond 208 hr, the differences between M5, M6, and M1 are all relatively minor (cf. figs. 7 and 14).

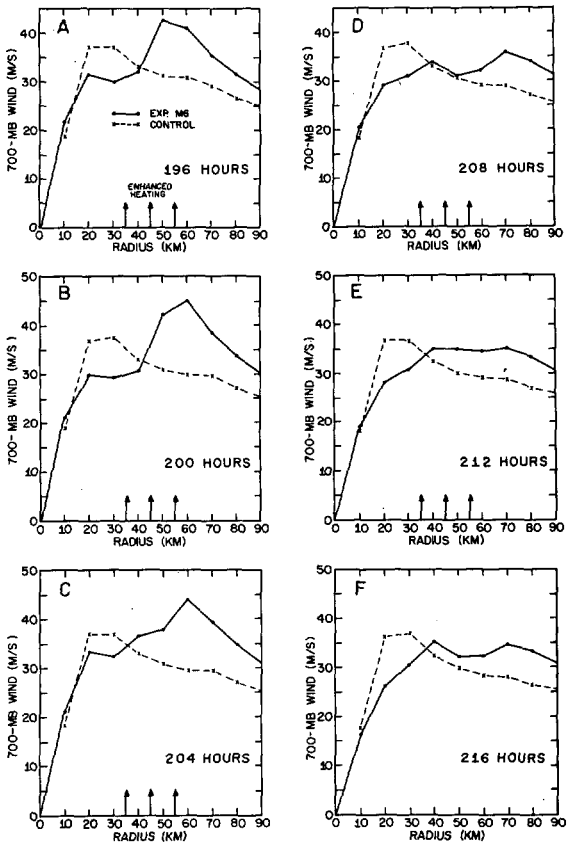

FIGURE 15.—Comparisons of 700-mb wind profiles for experiment M6 and the control experiment as a function of time.

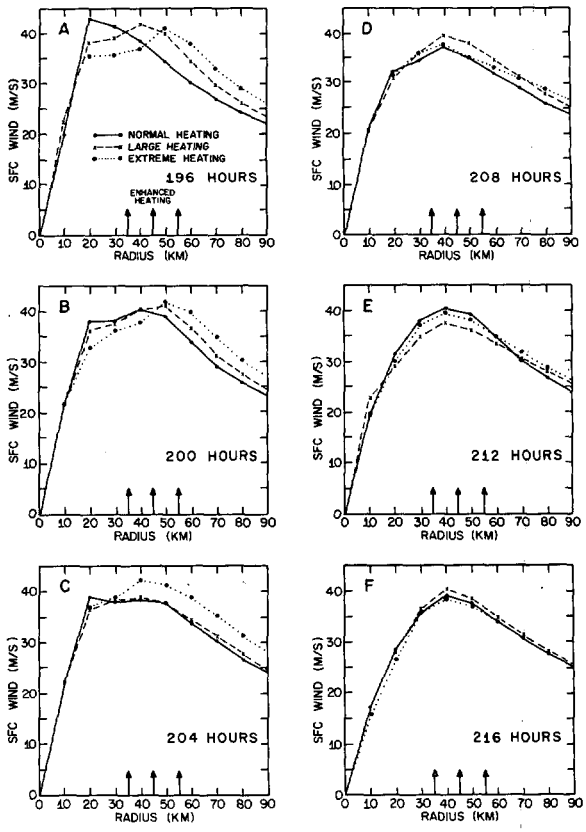

FIGURE 16.—Comparisons of surface wind profiles for normal, large, and extreme continuous heating at large radii; arrows indicate the grid points at which enhanced heating is applied.

The 700-mb winds obtained from experiment M6 (fig. 15) show the original maximum to be rapidly destroyed and to be replaced by a new maximum at a larger radius within the first 4 hr of the enhanced heating. The latter quickly intensifies and continues to intensify until the enhanced heating is terminated at 202 hr. Thereafter, it weakens rapidly; and by 212 hr, a new and fairly stable configuration is reached (figs. 15E and 15F). The behavior of the central pressure in experiment M6 is no more dramatic than that found for the experiments discussed previously.

Figure 16 depicts a comparison of experiments with normal, large, and extreme heating. In each case, enhanced heating is continuous and at large radii. Prior to 204 hr, the large heating calculation shows itself to be a transistion between the normal and extreme cases. After this time, the solutions in all experiments tend to oscillate; and no clear-cut relationship between heating rate and response is apparent. By 216 hr (fig. 16F), differences between the three experiments have virtually disappeared.

Figure 17 shows a comparison of experiments with continuous and intermittent heating at the extreme rate and at large radii. Differences of the type observed during the early hours are to be expected since (e.g., at 196 hr, fig. 17A) the experiment with continuous heating has been enhanced for a full 4 hr in comparison to only 2 hr in the intermittent case. By 212 hr, however, differ-

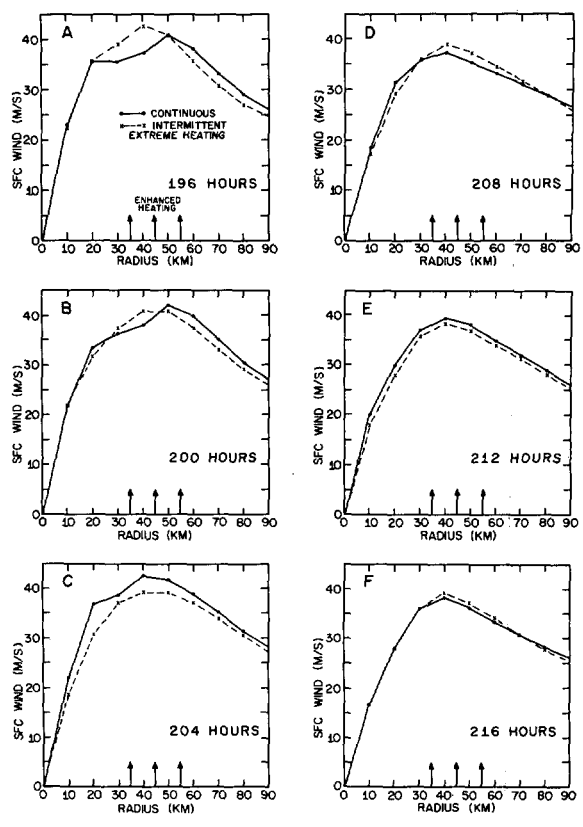

FIGURE 17.—Comparison of surface wind profiles for extreme continuous and intermittent heating at large radii; arrows indicate grid points at which enhanced heating is applied.

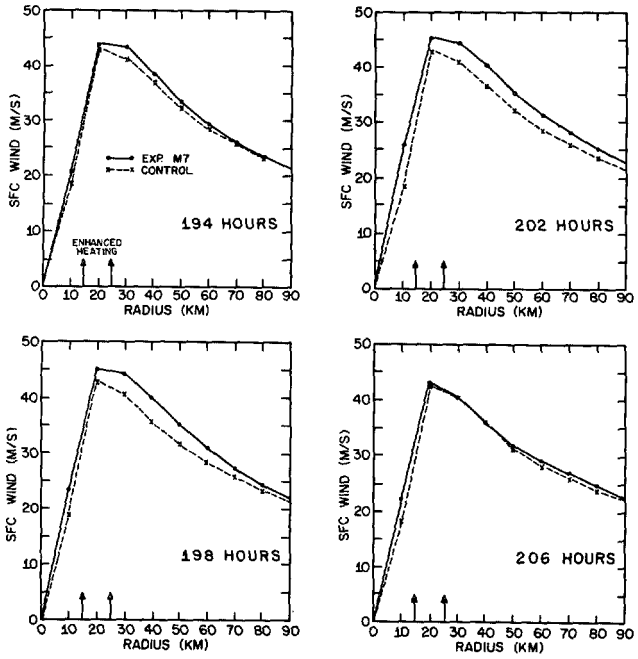

FIGURE 18.—Comparison of surface wind profiles for experiment M7 and the control experiment as a function of time; arrows indicate grid points at which enhanced heating is applied.

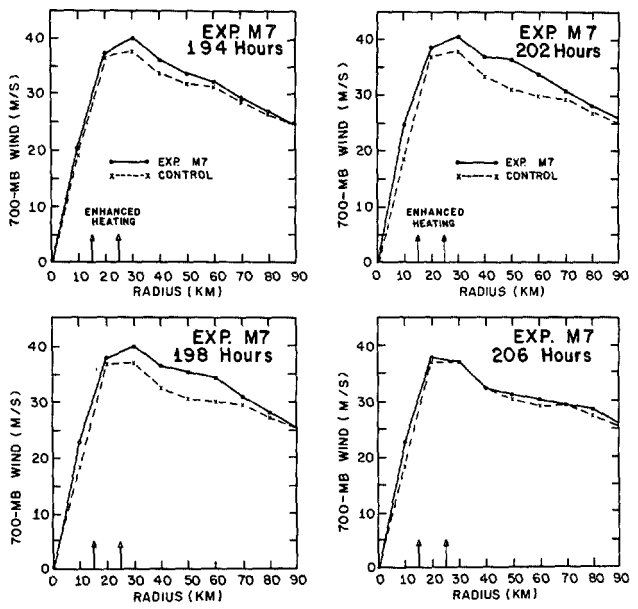

FIGURE 19.—Comparison of 700-mb wind profiles for experiment M7 and the control experiment as a function of time; arrows indicate grid points at which enhanced heating is applied.

ences between the two calculations have all but disappeared. At the normal and large heating rates and for enhanced heating at small radii, the differences between calculations with continuous and intermittent heating were even less than those shown by figure 17.

8. INTENSIFICATION OF THE SURFACE WIND MAXIMUM THROUGH ENHANCED HEATING

In section 1, it was suggested that enhanced heating at radii smaller than that of the surface wind maximum should tend to intensify the storm. Experiment M7 discussed here contains continuous extreme enhanced heating at radii of 15 and 25 km. If the arguments of section 1 are valid (cf. figs. 3 and 4), this should strengthen the surface wind maximum. Figures 18 and 19 show the deviations from the control to be in the sense anticipated, but to be surprisingly small. Recovery to a state near the control is rather rapid when the seeding is terminated at 202 hr. On the scale used for plotting figures 18 and 19, this experiment cannot be delineated from the control at and beyond hour 208.

The histories of the surface and 700-mb wind maxima as well as that of the central pressure (fig. 20) clearly show a direct response to the enhanced heating. However, the departure of the wind maxima from the control is never more than 2.5 to 3 m/s. At 700 mb, the increase in the wind maximum is less than the temporary increases found for the cases of "unfavorable" heating.

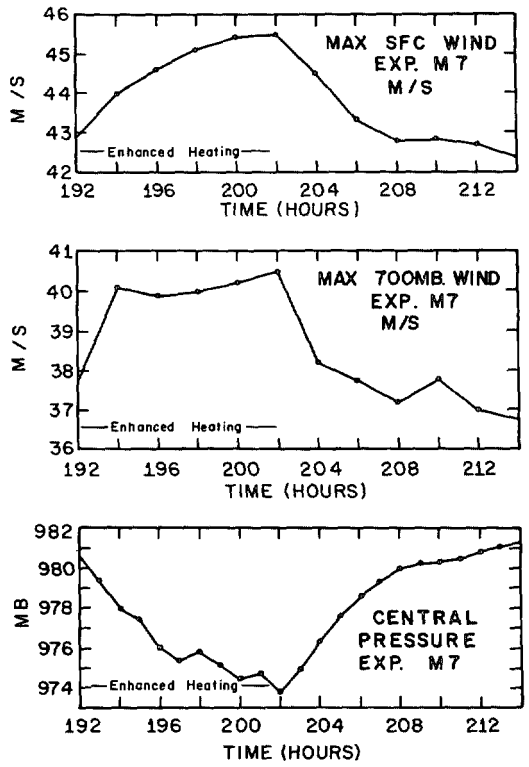

FIGURE 20.—Results from experiment M7.

Detailed examination of the response of experiment M7 reveals some fairly interesting points. From figure 21, the only significant changes in surface pressure gradient occur between radii of 5 and 15 km; and these have all but disappeared by 208 hr. The 500-mb temperature changes, even at the seeded radii, are less than 1°C,

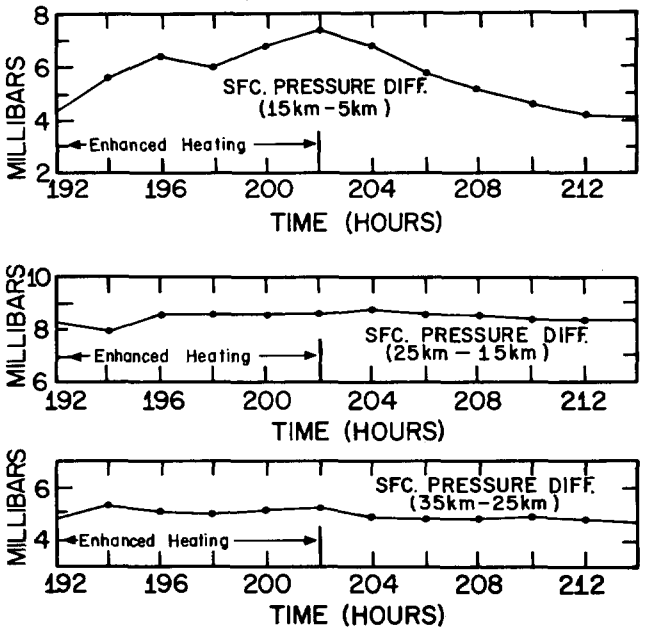

FIGURE 21.—Results from experiment M7; time histories of differences in surface pressure.

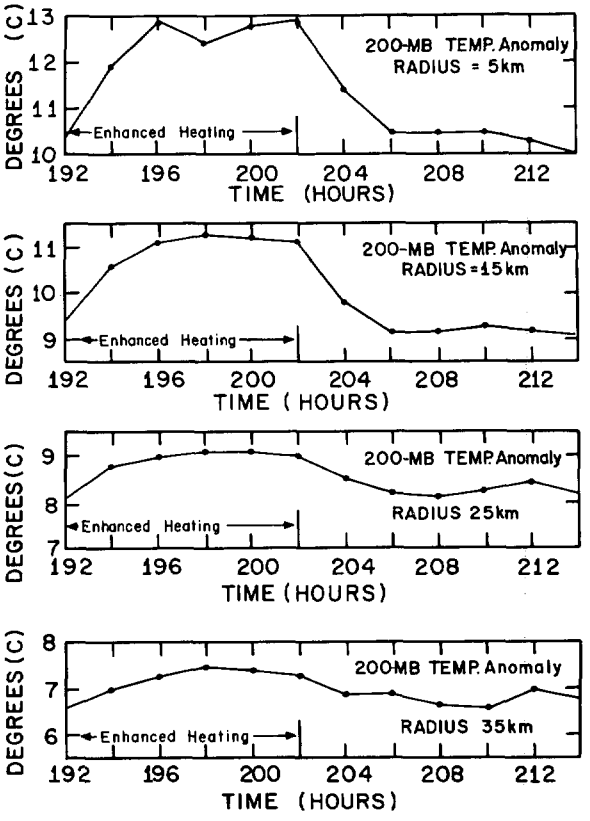

FIGURE 22.—Results from experiment M7; time histories of 200-mb temperature anomalies.

apparently due to a rapid response in the macroscale vertical motion that, in turn, provides sufficient adiabatic cooling to compensate for the enhanced heating. At 300 mb, the most notable temperature increase is at a radius of 25 km and is only about 1°C. This tends to weaken temperature gradients inward of 25 km and strengthen them at larger radii. It is therefore apparent that the changes of surface pressure gradient are not primarily reflections of temperature changes at either 300 or 500 mb. The former appear to be most strongly related to temperature changes (fig. 22) at 200 mb, which is fairly surprising since enhanced heating was not applied at this level. Even more surprising is the fact that the largest 200-mb warming occurs at 5 km which is outside the radial interval at which enhanced heating was applied.

Careful study of the control experiment at hour 192 indicates that the 200-mb temperature at 5 km is largely controlled by weak subsidence in a region of large static stability (fig. 23A) and small amounts of convective heating (note upward 900-mb vertical motion at 192 hr, fig. 23B) in a near-balance with the cooling effect of lateral mixing. Now at both 200 and 300 mb, the vertical motion at 5 km (fig. 23) responds to the enhanced heating with first a rapid upward surge and then with subsidence that strengthens until the enhanced heating is terminated at 202 hr. Thereafter, the vertical motion recovers rapidly to values near that of the control.

These variations of vertical motion are related to a significant increase of vertical mass transport in the region of enhanced heating (fig. 24). Apparently, the upper troposphere, at least partially, compensates for this increased mass transport with an increased inflow. This, in turn, is associated with the development of the

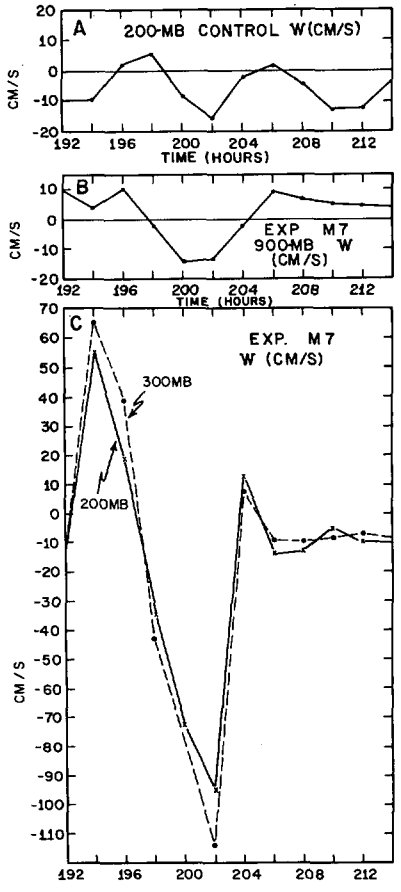

FIGURE 23.—Vertical motions at 5-km radius.

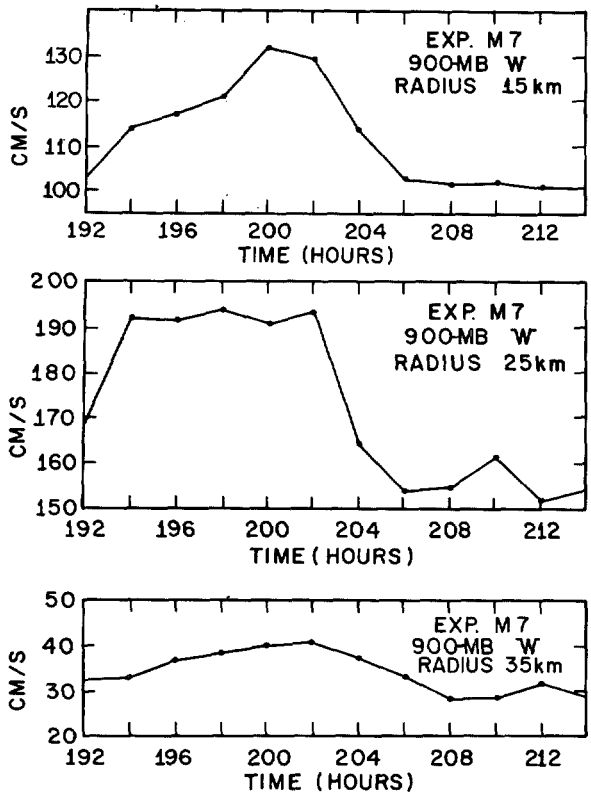

FIGURE 24.—Vertical motions at 900 mb for experiment M7.

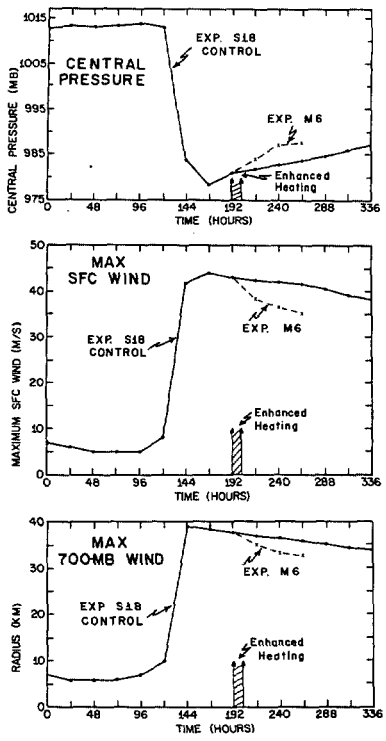

FIGURE 25.—Comparisons of experiment M6 with the control experiment.

intense downdraft at the 5-km radius already noted above. The latter ultimately reaches all the way into the boundary layer (fig. 23B).

The 200-mb temperature increases at 5 km are undoubtedly related to this subsidence. What is less clear, however, is the lack of a similar warming at 300 mb as well as the absence of cooling at 200 and 300 mb with the increased ascent during the first 4 hr of the calculation. This appears partially explicable by differences in static stability. For descent, the 200-mb static stability is about twice as great as the 300-mb value. Since the model employs upstream differencing, static stability is also dependent on the direction of the vertical motion. At 200 mb, the static stability for upward motion is about half of that for downward motion; at 300 mb, the stability for upward motion is about 25 percent greater than for downward motion.

9. LONG-TERM ASPECTS OF EXPERIMENT M6

The experiments discussed in sections 5, 6, and 7 appear to reach fairly stable configurations by the time the calculations are terminated at 216 hr. For examining this point further, experiment M6 (extreme continuous heating at large radii) was continued for an additional 48 hr. Radial profiles of surface and 700-mb wind at 240 and 264 hr (not shown) confirm that the modified configuration is, indeed, quite stable. At 264 hr, the surface wind maximum for the modified storm (fig. 25) is still over 6 m/s less than that of the control.

It is not our intention to imply that such highly stable modified configurations can be achieved in the real atmosphere where the interactions with adjacent synoptic situations are of major importance and where variations of sea conditions as well as feedbacks between ocean and atmosphere play significant roles.

10. COMMENTS ON THE ENERGETICS OF CONTINUOUS NORMAL HEATING AT LARGE RADII

Upon reading a first draft of this manuscript, one of the author's colleagues raised a rather basic set of questions. Comparison of wind profiles for seeded and control storm (e.g., fig. 7) strongly suggests that the kinetic energy content of the seeded storm is greater than that of the control. If this is indeed so, the question of the source of this additional energy immediately arises. Can it be taken into account by the artificial enhancement of the heating? Is the efficiency (ratio of the rate of kinetic energy production to the rate of latent heat release) significantly different for the seeded storm?

Unfortunately, history tapes for the experiments previously described had not been preserved. Therefore, an additional experiment with continuous normal heating at large radii was carried out. The control experiment S35 for the new calculation is (in the mature stage) quite similar to the control previously used (figs. 1 through 6).

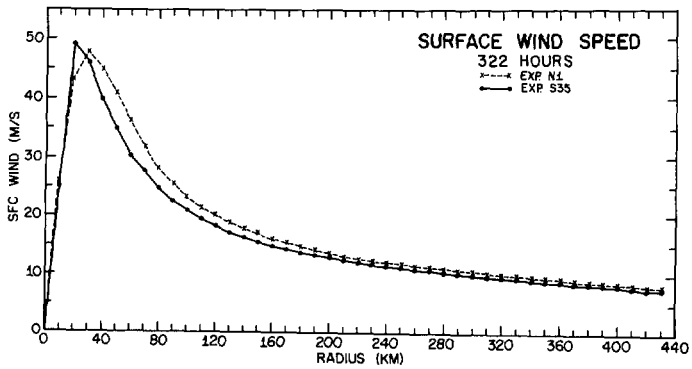

FIGURE 26.—Results from experiment N1; comparison of the surface wind profile with control experiment S35 at the termination of seeding (322 hr).

TABLE 1.—*Kinetic energy content (kilojoules) of the control (exp. S35, top) and the seeded storm (exp. N1, bottom)*

Time (hours)	0- to 100-km radius ($\times 10^{14}$)	0- to 200-km radius ($\times 10^{14}$)	0- to 400-km radius ($\times 10^{14}$)
312	1.17	2.10	3.23
324	1.16	2.11	3.29
336	1.15	2.10	3.32
312	1.17	2.10	3.23
324	1.42	2.56	3.91
336	1.35	2.47	4.00

TABLE 2.—*Percentage difference in kinetic energy between the control (exp. S35) and the seeded storm (exp. N1)*

Time (hours)	0- to 100-km radius	0- to 200-km radius	0- to 400-km radius
324	22	21	19
336	17	18	20

Experiment S35 reached a steady state approximating that of S18 between 312 and 336 hr. Heating enhancement at the normal rate was then imposed for the 10-hr period 312 through 322 hr. This calculation is designated experiment N1.

Figure 26 compares the surface wind profile for experiment N1 with that of the control at 322 hr. Note that the radial scale is half that shown on figures previously discussed and, further, that the profile is shown for the entire range of the computational domain. Table 1 shows a comparison between the kinetic energy content of the control and seeded storm at 312, 324, and 336 hr while table 2 shows the percentage difference of kinetic energy between the two storms. Clearly, the seeded storm contains about 20 percent more kinetic energy than does the control.

TABLE 3.—*The 12-hr averages of the time rate of change of kinetic energy* (kJ/s) *for the control (exp. S35, top) and the seeded storm (exp. N1, bottom) centered on the indicated time*

Time (hours)	0- to 100-km radius	0- to 200-km radius	0- to 400-km radius
318	-2.67×10^{7}	2.55×10^{7}	1.50×10^{8}
330	-5.71×10^{6}	-1.67×10^{7}	6.71×10^{7}
318	5.83×10^{8}	1.07×10^{9}	1.58×10^{9}
330	-1.64×10^{8}	-2.14×10^{8}	1.97×10^{8}

TABLE 4.—*Contribution of the total release of latent heat to the enthalpy budget* (kJ/s) *for the control (exp. S35, top) and the seeded storm (exp. N1, bottom) averaged over the 12-hr interval centered on the indicated time*

Time (hours)	0- to 100-km radius ($\times 10^{11}$)	0- to 200-km radius ($\times 10^{11}$)	0- to 400-km radius ($\times 10^{11}$)
318	1.95	2.20	2.43
330	1.85	2.04	2.36
318	2.38	2.60	3.04
330	2.63	2.73	3.16

TABLE 5.—*Efficiency (%) of the control experiment S35 and the seeded storm N1. Values are appropriate to the radial interval 0–200 km and are 12-hr averages centered on the indicated time.*

Time (hours)	Exp. S35	Exp. N1
318	3.69	3.35
330	3.94	3.38

Table 3 shows 12-hr averages of the time rate of change of kinetic energy centered at the indicated hour. For most cases, the changes in the seeded storm are an order of magnitude greater than those of the control and, hence, are a rough measure of the thermal energy input required to obtain the kinetic energy changes noted in the modified storm provided that the efficiency was 100 percent and all other factors were equal which, of course, is not the case.

The artificial heating enhancement from 312–322 hr works out to be 1.69×10^{10} kJ/s which is well over an order of magnitude greater (table 3) than that required to balance the kinetic energy increase between the modified and control systems. An extremely interesting result is revealed by table 4 which shows a comparison of the 12-hr averages of total latent heat released for the modified and unmodified systems (note that for the modified storm the artificial enhancement is entirely within the inner 100 km of the storm and is at the rate of 1.69×10^{10} kJ/s). We note (even if the enhancement rate is subtracted out in the inner 100 km at 318 hr) that the latent heat release (and, hence, the rainfall) is substantially larger in the modified system. This, of course, indicates that the arti-

ficial heating was not only effective in itself but, further, that its presence induced an increase in natural rainfall and that this is particularly true of the outer regions of the storm. As a result, despite the larger kinetic energy content of the modified storm, the efficiency (table 5) of the seeded storm is somewhat less than that of the control. [The budget code for this model, as applied in previous publications (Rosenthal 1969, 1970*a*, 1970*b*), calculates efficiencies only for the radial interval 0–200 km. Therefore, values for other radial intervals are not available.]

REFERENCES

Gentry, R. Cecil, "Project STORMFURY," *Bulletin of the American Meteorological Society*, Vol. 50, No. 6, June **1969**, pp. 404–409.

Gentry, R. Cecil, "Hurricane Debbie Modification Experiments, August 1969," *Science*, Vol. 168, No. 3930, Apr. 24, **1970**, pp. 473–475.

Hawkins, Harry F., "Comparison of Results of the Hurricane Debbie (1969) Modification Experiments With Those From Rosenthal's Numerical Model Simulation Experiments," *Monthly Weather Review*, Vol. 99, No. 5, May **1971**, pp. 427–434.

Rosenthal, Stanley L., "Numerical Experiments With a Multilevel Primative Equation Model Designed to Simulate the Development of Tropical Cyclones: Experiment I," *ESSA Technical Memorandum* ERLTM-NHRL 82, U.S. Department of Commerce, National Hurricane Research Laboratory, Miami, Fla., Jan. **1969**, 36 pp.

Rosenthal, Stanley L., "Experiments With a Numerical Model of Tropical Cyclone Development—Some Effects of Radial Resolution," *Monthly Weather Review*, Vol. 98, No. 2, Feb. **1970***a*, pp. 106–120.

Rosenthal, Stanley L., "A Circularly Symmetric Primitive Equation Model of Tropical Cyclone Development Containing an Explicit Water Vapor Cycle," *Monthly Weather Review*, Vol. 98, No. 9, Sept. **1970***b*, pp. 643–663.

Simpson, Robert H., and Malkus, Joanne S., "Experiments in Hurricane Modification," *Scientific American*, Vol. 211, No. 6, Dec. **1964**, pp. 27–37.

[*Received June 10, 1970; revised September 21, 1970*]